

EFFICIENT ELECTRON TRANSFER REACTION
CATALYZED BY SYNTHETIC Fe-S CLUSTER IN MICELLES:
ITS KINETIC BEHAVIOR AND COMPARISON WITH NATURAL FERREDOXIN.

Iwao Tabushi[†], Yasuhisa Kuroda^{*}, Yoro Sasaki

Department of Synthetic Chemistry, Kyoto University,
Yoshida Sakyo-ku, Kyoto 606, Japan

(Received in Japan 11 January 1988)

Abstract - Detailed kinetics of the electron transfer reaction catalyzed by the synthetic iron-sulfur cluster, (3), in cetyltrimethylammonium bromide micelles were investigated. The rates of the reduction of N-9-acridinyl-pivalamide, (5), showed the clear saturation behaviors both for the concentrations of dithionite (electron donor) and 5 (final electron acceptor). The results demonstrate that the reaction implies the pre-equilibrium of these two species during the electron transfer. The detailed analysis of the concentration dependencies gave the necessary kinetic parameters, which indicated that the both processes of electron transfer reactions in the present system, $\text{SO}_2^{2-} + \underline{3}^{2-} \longrightarrow \underline{3}^{3-}$ and $\underline{3}^{3-} + \underline{5}_{\text{ox.}} \longrightarrow \underline{3}^{2-} + \underline{5}_{\text{red.}}$, showed almost the same efficiencies with those of native ferredoxins.

Introduction

Ferredoxins, which contain one or two non-heme iron-sulfur clusters as an active site, play unique and important roles as electron transfer catalysts in the biological systems such as respiration, photosynthesis, nitrogen fixation, hormone synthesis and sulfur and carbon metabolism.¹⁾

After the Holm's beautiful preparations of the synthetic complexes $[\text{Fe}_4\text{S}_4(\text{SR})_4]^{2-}$ which are true analogs of the active sites of bacterial iron-sulfur proteins,²⁾ many these types of iron-sulfur clusters have been synthesized as models of the active sites of ferredoxins and their structural, spectroscopic, magnetic and electrochemical characteristics have been elucidated.³⁾ The attempts to apply such synthetic iron-sulfur clusters to electron transfer catalysts in organic solvents⁴⁾ or liquid membrane system⁵⁾ have been also reported. Although many important knowledges on the iron-sulfur clusters have been accumulated through these extensive investigations, there is little success⁶⁾ of the application of the synthetic iron-sulfur cluster to the electron transfer catalyst in an aqueous solution because of their instability in water,⁷⁾ which is quite contrary to that of the native ferredoxin.⁸⁾ Recently we reported that both of the oxidized and reduced forms of the synthetic iron-sulfur cluster (3) showed fairly good stability in cetyltrimethylammonium bromide (CTAB) micelles,⁹⁾ and that 3 in CTAB micelles was reduced by dithionite ion reasonably fast and could successfully catalyze the electron transfer reaction between dithionite and

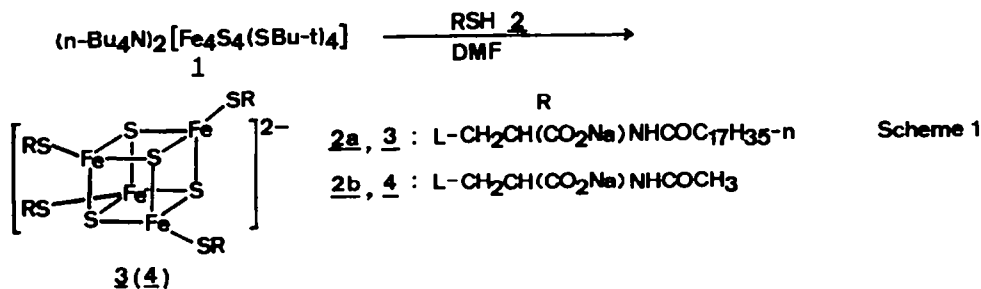
[†] Deceased on March 22, 1987.

acridine derivatives in water.¹⁰⁾ In this paper, we wish to report the detailed kinetics of 3/CTAB-catalyzed electron transfer reaction between dithionite and acridine derivatives.

Results and Discussion

Spectral Properties of Fe-S Clusters, 3 and 4

The Fe-S cluster 3 was prepared by the ligand exchange reaction¹¹⁾ starting from $(n\text{-Bu}_4\text{N})_2[\text{Fe}_4\text{S}_4(\text{SBu-t})_4]$ ¹²⁾ (see Scheme 1). The compound 4 was also prepared by the same method and used as a reference hydrophilic cluster to make a



comparison of the stability in water and the electronic spectrum. As shown in Fig. 1(a), the compound 3 and 4 showed the characteristic electronic absorption spectra of Fe₄S₄ clusters in DMF. A cetyltrimethylammonium bromide (CTAB) micellar solution of 3 (pH 8.5) showed electronic absorptions at 300 nm (ϵ , 2.2×10^4) and 396 nm (ϵ , 1.7×10^4) (Fig. 1(b)). As previously reported,¹²⁾ the significant blue shift by the solvent change from DMF to water was observed

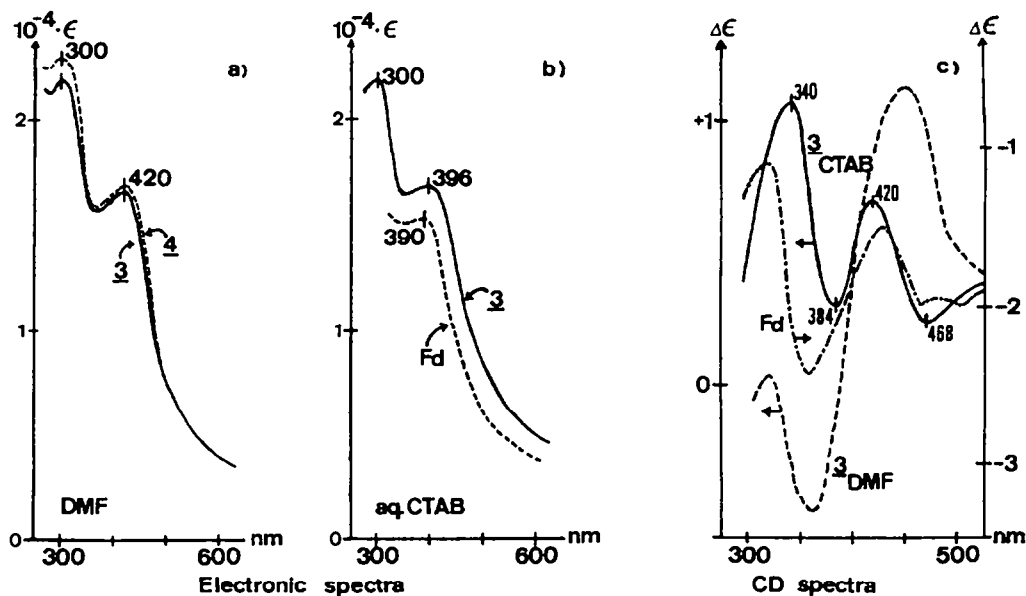


Figure 1. Electronic and CD spectra of 3, 4 and native ferredoxin.¹³⁾ a) in DMF, [3]=0.1mM, [4]=0.1mM. b) in aq. CTAB micelles, [3]=0.1mM, [CTAB]=20mM in 100mM Tris-Cl buffer at pH 8.5. c) in DMF, [3]=0.1mM, and in aq. CTAB micelles, [3]=0.1mM, [CTAB]=20mM in 100mM Tris-Cl buffer at pH 8.5.

especially for the 396 nm band and these observations suggest that the present Fe_4S_4 core part of 3 locates near the surface polar region of micelles rather than the hydrophobic core of micelles.

Since the present Fe-S clusters, 3, has optical active L-cysteine ligands, 3 is active for CD spectra as shown in Fig. 1(c). CD spectra of 3 in DMF and micelles are significantly different and these results indicate the large difference of the configurational surroundings around Fe-S cluster between these solvent systems. Although the detailed identifications of CD spectra of native ferredoxin (and also synthetic Fe-S clusters) are not known yet, it should be noted that CD extrema of 3 at 340, 384, 420, 468 and 530 nm in the micellar solution were very similar to those of native ferredoxin from *Bacillus stearothermophilus* which contained one Fe_4S_4 core (see Fig. 1(c)).

Stabilities of Fe-S Clusters in Aqueous Micellar Solutions

The stabilities of 3 and 4 in DMF and aqueous CTAB micellar solutions were investigated by following the decrease of its characteristic electronic absorption at 396 nm. As shown in Table 1, the pseudo first order hydrolytic decomposition rate ($k_{\text{dec.}}$) of 4 was very fast ($k_{\text{dec.}} = 2.6 \text{ s}^{-1}$) even in 10% H_2O -90% DMF at pH 8.5. In contrast with this, that of 3 in aqueous micellar solution (CTAB 20mM) at pH 8.5 was $1.4 \times 10^{-7} \text{ s}^{-1}$, being ca. 2×10^7 fold slower than that of 4 (in 10% H_2O -90% DMF) and comparable to that of native ferredoxin⁸⁾ (see Table 1). It should be noted that, based on these observations, the present cluster, 3 was safely concluded to be *completely* bound into the CTAB micelles under the present conditions.

Table 1. Decomposition rates of Fe_4S_4 Clusters

Fe_4S_4 Cluster	$k_{\text{dec.}}$ (s^{-1})	condition
<u>3</u>	1.4×10^{-7} a)b)	pH 8.5, 25°C
<u>4</u>	2.6 a)c) (1.4×10^{-6}) a)b)	pH 8.5, 25°C
<i>C. aciduriaci</i> Fd	0.4×10^{-7} d)	pH 7.4, 4°C
<i>C. vinosum</i> Fd	1.0×10^{-6} e)	pH 8.0, 30°C

a) Based on the characteristic absorption changes of 3 and 4 at 396 nm.

b) 0.1 mM Fe-S cluster, 20 mM CTAB, 100 mM Tris-Cl

c) 90% DMF-10% H_2O , 10mM Tris-Cl d) ref. 8b) e) ref. 8c)

Since it is interesting to compare the stabilizing effect of the different micellar systems, the stabilities of 3 in the sodium dodecylsulfate (SDS) and Triton X-100 micelles are also investigated. The hydrolytic decomposition rates of 3 in the SDS micelles (SDS, 50 mM) and the Triton X-100 micelles (Triton X-100, 10% v/v) at pH 8.5, 25°C were $1.3 \times 10^{-4} \text{ s}^{-1}$ and over $4 \times 10^{-4} \text{ s}^{-1}$, respectively, which were ca. 10^3 times larger than that in the CTAB micelles. Thus, the results made the sharp contrast with that previously reported by Tanaka et. al., where the synthetic cluster, $[\text{Fe}_4\text{S}_4(\text{SC}_6\text{H}_4\text{C}_8\text{H}_{17})_4]^{2-}$, was stable not only in cetyltrimethylammonium chloride but also in SDS and Triton X-100 micelles.¹⁴⁾ This sharp difference between stabilities of 3 and $[\text{Fe}_4\text{S}_4(\text{SC}_6\text{H}_4\text{C}_8\text{H}_{17})_4]^{2-}$ in these micelles suggests that the Coulombic interaction between cationic micelles and negative charge (-6) of the present cluster, 3, is more important for the binding into the micelles and stabilization of the cluster than the hydrophobic interaction between

micelles and long alkyl chains of 3. On the other hand, in the case of $[\text{Fe}_4\text{S}_4(\text{SC}_6\text{H}_4\text{C}_8\text{H}_{17})_4]^{2-}$, the cluster was strongly bound only by the hydrophobic interaction because of its small negative charge (-2). The importance of the Coulombic interaction between the micelles and the present cysteine ligand cluster is also suggested by the fact that even 4 having more hydrophilic N-acetylcysteine ligands is significantly stabilized in CTAB micelles, though its decomposition rate is $1.4 \times 10^{-6} \text{ s}^{-1}$, which is 10 times faster than that of 3 in CTAB micelles (see Table 1).

Redox Potentials of Fe-S Clusters and Substrate in Aqueous Micellar Solutions

The redox potentials ($E^{1/2}$) of 3 and 4 in DMF containing 0.1N n-Bu₄NBr were measured by a cyclic voltammetry to be -1.08 V and -1.10 V vs Ag/AgCl (-0.88 V and -0.90 V vs NHE) at 25°C, respectively, which lie in the reasonable range of usual Fe₄S₄ type clusters having alkylthiolate ligands.¹⁵⁾ In contrast, the $E^{1/2}$ of 3 in the aqueous CTAB micellar solution containing 0.1M of KCl (pH 8.5) was found to be -0.75 V vs Ag/AgCl (-0.55 V vs NHE) (see Fig. 2(a)), which was close to that of native ferredoxin (-0.24 - -0.49 V vs NHE).¹⁾ The observed positive potential shift of 3 by the solvent change from DMF to H₂O (0.33 V) was similar to those of other synthetic cluster which were measured in aqueous solution containing large excess of mercaptans¹²⁾ or in micelles.¹⁴⁾

Since the reduction potential of N-9-acridinyl-pivalamide, 5, which was employed as the substrate in this work, under the micellar conditions was not known, the value was also determined by the cyclic voltammograms.¹⁰⁾ Interestingly, the reduction potential of 5 also showed the significant positive reduction potential shift by the solvent change from DMF, -0.80 V vs NHE, to the aqueous micellar solution, -0.51 V vs NHE (Fig. 2(b)). Thus, the result suggested that the hydration around both of 3 and 5 were similar each other and the locations of the Fe₄S₄ core of 3 and 5 were also similar in the CTAB micelles.

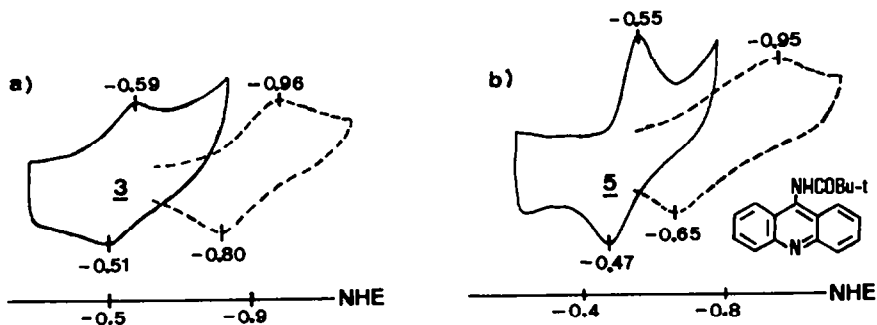


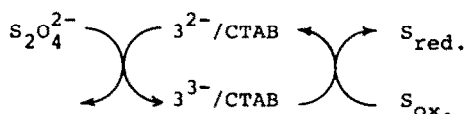
Figure 2. Cyclic voltammetry of 3 and N-9-acridinyl-pivalamide. a) 3, (—) in aq. CTAB micelles, [CTAB]=5mM, [KCl]=100mM in 100mM Tris-Cl buffer at pH 8.5, (----) in DMF, [n-Bu₄NBr]=100mM. b) N-9-acridinyl-pivalamide, (—) in aq. CTAB micelles, [CTAB]=5mM, [KCl]=100mM in Tris-Cl buffer at pH 8.5, (----) in DMF, [n-Bu₄NBr]=100mM.

Electron Transfer Reaction Catalyzed by 3 in Micelles

As previously reported,¹⁶⁾ the present cluster, 3, in CTAB micelles showed the reasonable electron uptake ability from S₂O₄²⁻ in the bulk aqueous solution. The detailed kinetic analysis reveals that the electron transfer reaction from S₂O₄²⁻ to 3 proceeds through the non-cooperative multiple binding of S₂O₄²⁻ onto the surface of CTAB micelles and following dissociation of S₂O₄²⁻ to SO₂⁻ which is

actual reducing species. The kinetic parameters obtained are 19 ± 7 for the maximum number of $S_2O_4^{2-}$ bound on the one micellar particle (n), $1300 \pm 400 M^{-1}$ for the single binding constant (K_1) and $18 \pm 3 s^{-1}$ for the specific intramolecular reduction constant of 3 by $SO_2^{\cdot -}$ in the micelles (k_1),¹⁷⁾ respectively. Although it is difficult to directly compare the electron uptake abilities of present $\underline{3}$ /CTAB with that of native ferredoxin because such a binding process of $S_2O_4^{2-}$ is not known for native ferredoxin, the overall electron transfer rates from $S_2O_4^{2-}$ to Fe-S cluster cores are shown to be very similar each other in these systems (see the later section).

Thus, the electron transfer reaction catalyzed by $\underline{3}$ was surveyed by changing



Scheme 2

the reduction potential of substrates (S)¹⁰⁾ (Scheme 2). The results clearly showed that compounds having slightly higher reduction potentials than that of $\underline{3}$ ($-0.55 V$ vs NHE), such as N-9-acridinyl-amide derivatives are suitable as the final electron acceptors in the successive electron transfer reactions catalyzed by $\underline{3}$. Otherwise the direct electron transfer from $S_2O_4^{2-}$ proceeds too quickly and dominates the overall electron transfer reaction, as observed for anthraquinone derivatives which have too high reduction potentials or no practical electron transfer occurs as observed for 9-alkylaminoacridine with too low reduction potential.

In order to elucidate the detailed kinetic process of these successive electron transfer reactions catalyzed by $\underline{3}$, dithionite reduction of N-9-acridinyl-pivalamide, which was the best substrate found was studied profoundly. The reactions were followed by decrease of its characteristic absorption intensity at 385 nm and independently fluorescence intensity at 450 nm (excit. 360 nm).¹⁰⁾ The typical reaction traces of the fluorescence measurements were shown in Fig 3.

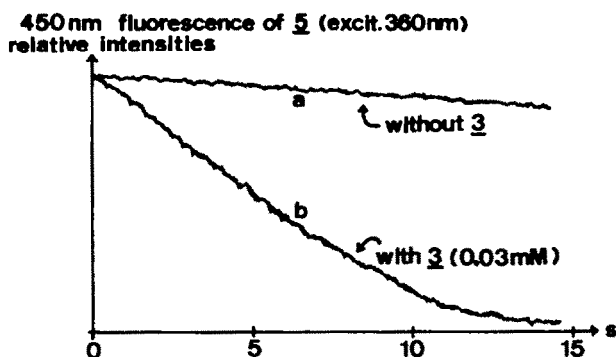


Figure 3. Typical reaction traces of electron transfer reactions from $S_2O_4^{2-}$ to N-9-acridinyl-pivalamide ($\underline{5}$). $[\underline{5}] = 0.1mM$, $[\text{Disodium dithionite}] = 8mM$. a) without $\underline{3}$, $k_{obs.} = 0.83 \times 10^{-6} M \cdot s^{-1}$. b) with $\underline{3}$ ($0.03mM$), $k_{obs.} = 9.4 \times 10^{-6} M \cdot s^{-1}$.

Although the initial zero order traces of the reactions were employed for the present kinetic analysis, the reactions were confirmed independently to proceed without any appreciable side reaction, i.e., for example, after oxygen-oxidation of the reduction product of substrate ($\underline{5}$), over 98 % of $\underline{5}$ was recovered. Thus, the dependences of the initial zero order rate constants of the reduction of N-9-acridinyl-pivalamide ($\underline{5}$) on the concentrations of dithionite, $\underline{5}$ and $\underline{3}$ were investigated. All the rate constants were corrected by that without $\underline{3}$ (less than

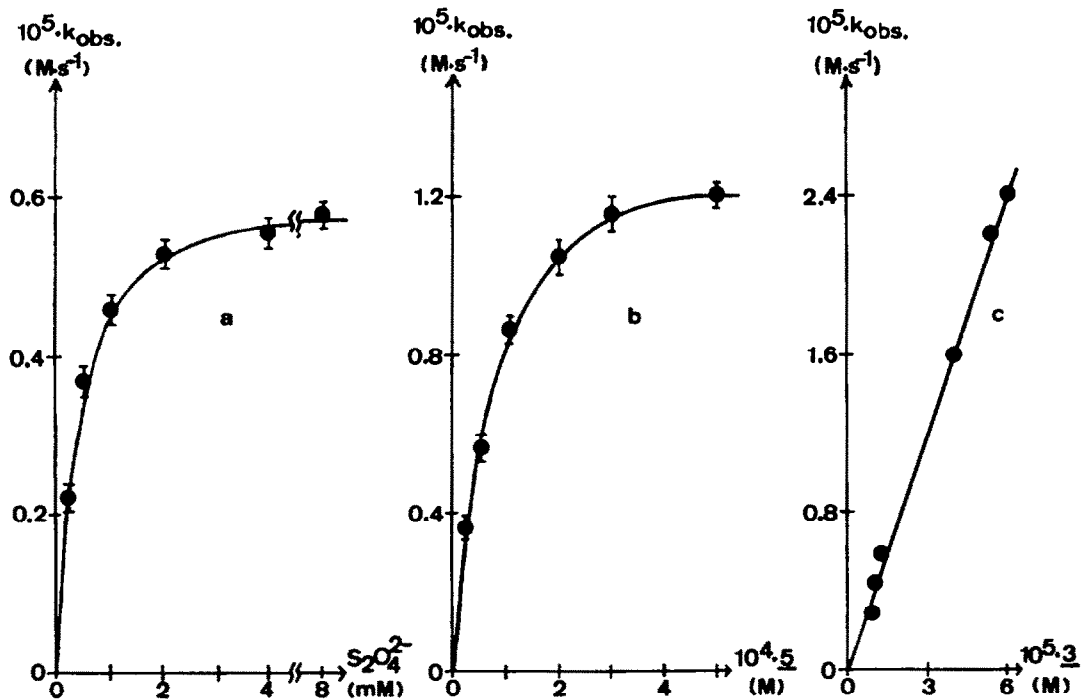


Figure 4. Variation of reduction rates (k_{obs} , $M \cdot s^{-1}$) of N-9-acridinyl-pivalamide (5) as functions of [dithionite], [5] and [3].

● ●; observed data, —; theoretical curves calculated from eq. 1.
 Line a: [5]=0.05mM, [3]=0.03mM. Line b: [dithionite]=8mM, [3]=0.03mM.
 Line c: [5]=0.5mM, [dithionite]=8mM, 5mM CTAB, 100mM Tris-Cl (pH 8.5, 25°C).

10 % even at the minimum concentration of 3) and summarized in Fig. 4. As clearly shown in Fig. 4(a), a saturation behavior for the concentration of dithionite was observed under the present conditions (5 0.05 mM, 3 0.03 mM, CTAB 5 mM, Tris-Cl 100 mM, pH 8.5), which was similar to that observed for the reduction of 3 with $S_2O_4^{2-}$ (16)

A saturation behavior for the concentration of substrate, 5, was also observed when the concentration of 5 increased from 0.025 mM up to 0.5 mM at the constant concentration of dithionite (8 mM) (see Fig. 4(b)). At the 0.03 mM of 3, the maximum reduction rate (V_{max}) of 5 was obtained to be $1.2 \times 10^{-5} M \cdot s^{-1}$ as a saturation rate. This saturation clearly suggests that the reaction, $\underline{3}^{3-} + \underline{5}_{ox} \rightarrow \underline{3}^{2-} + \underline{5}_{red}$, also proceeds through the binding process of 5 into CTAB micelles (see Fig. 5).

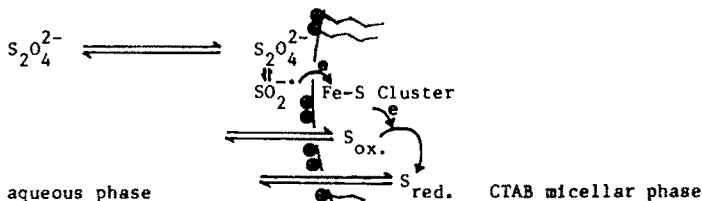
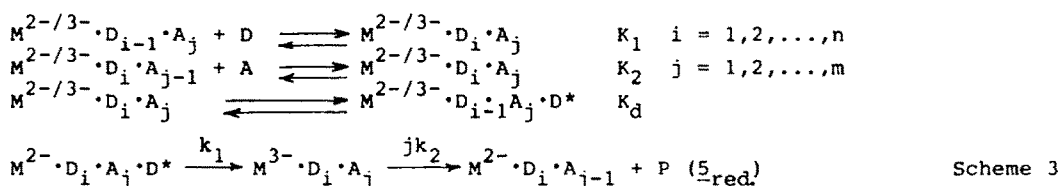


Figure 5. Electron transfer system of $[Fe_4S_4((L)-SCH_2CH(CO_2Na)NHCOC_{17}H_{35}-n)]^{2-/-3-}$

Finally the maximum reduction rates (V_{\max}) of 5 at 8 mM of $S_2O_4^{2-}$ and 0.5 mM of 5 was found to be proportional to the concentration of the catalyst, 3 (see Fig. 4(c)), which indicated again that the Fe-S cluster, 3, quantitatively incorporated into micelles and there was no appreciable equilibrium between 3 in the micelles and bulk solution. The maximum turnover frequency of 3 was obtained to be 0.4 s^{-1} as a slope of a line in Fig. 4(c). The highest turnover number of 3 observed in the present electron transfer reaction system was 28 (mol product/mol cat) which was obtained under the conditions, $[S_2O_4^{2-}] = 8 \text{ mM}$, $[5] = 0.5 \text{ mM}$ and $[3] = 0.012 \text{ mM}$. Based on these observations, the following reaction scheme is derived as the most probable mechanism for the present reaction, where the random non-cooperative binding of dithionite ion and 5 into the CTAB micelles were implied.



where $M^{2-/3-}$ is micelles including 3, D is dithionite, D^* is $SO_2^{\cdot-}$ radical anion, A is substrate (5), P is reduced A and n and m are maximum numbers of bound D and A on micelles, respectively.

Assuming the steady state concentration of M^{3-} , the observed initial rate constant ($M \cdot s^{-1}$) is given by eq. 1 (see Appendix for the details).

$$k_{\text{obs}} (M \cdot s^{-1}) = \frac{C_T k_1 (nK_1 K_d D_f / M_T)^{1/2} k_2 m K_2 A_f}{k_1 (nK_1 K_d D_f / M_T)^{1/2} (1 + K_2 A_f) + k_2 m K_2 A_f (1 + K_1 D_f)^{1/2}} \quad \text{eq. 1}$$

where D_f and A_f are concentrations of free D and A,¹⁸⁾ M_T is total micellar concentration,¹⁹⁾ and C_T is total micellar concentration containing 3. The computer aided nonlinear least square calculation for all the data shown in Fig. 4 (a-c), using known value of $K_d = (1.4 \pm 0.4) \times 10^{-9} M$,²⁰⁾ $n = 19 \pm 7$, $K_1 = 1300 \pm 400 \text{ M}^{-1}$ and $k_1 = 18 \pm 3 \text{ s}^{-1}$,¹⁶⁾ gave the necessary parameters to be 4.4 ± 0.4 for m, $5550 \pm 460 \text{ M}^{-1}$ for K_2 and $0.82 \pm 0.05 \text{ s}^{-1}$ for k_2 , respectively (see Fig. 4). The equilibrium constant of mK_2 was also confirmed by independent experiments of static absorption change (360 nm) of 5 ($4.3 \times 10^{-5} \text{ M}$) at various concentrations of CTAB micelles (CTAB 5-15 mM). The double reciprocal plots of the changes of absorption intensities against the concentration of micelles¹⁹⁾ gave the mK_2 value to be $(2.0 \pm 0.4) \times 10^4 \text{ M}^{-1}$, which was in a reasonable agreement with that obtained from above kinetic analysis.

Comparison of Fe-S Cluster/CTAB Micelle and Native Ferredoxin

As shown in Table 2, the reduction rate (k_{red}), $3^{2-} \rightarrow 3^{3-}$ by $SO_2^{\cdot-}$, is similar to that of natural ferredoxin. It is interesting to note that the apparent rate of the electron transfer ($k_2 K_2$) from 3/CTAB to 5 is also similar to that from ferredoxin to $Co(en)_3^{3+}$,²¹⁾ even though the thermodynamic driving force of the reduction ($\Delta E^{1/2}$) is favorable to the latter, e.g., $\Delta E^{1/2} (Co(en)_3^{3+} - Fd) = 0.16 \text{ V}$,²¹⁾ and $\Delta E^{1/2} (5 - \text{3/CTAB}) = 0.04 \text{ V}$, respectively (see Table 2). This efficient electron transfer of 3/CTAB, however, is evidently due to the present favorable binding constant (K_2) of 5 compared with that of $Fd \cdot Co(en)_3^{3+}$ (597 M^{-1})²¹⁾ and the intramolecular electron transfer rate (k_2) of 3/CTAB lies in the same range with that of ferredoxin expected from its $\Delta E^{1/2}$ value. However, it should

be noted that, for the electron acceptor such as cytochrome c_3 which is known to form the tight 1:1 complex with ferredoxin, the extremely large rate is observed²²⁾ (see Table 2).

Table 2. Comparison of $\underline{3}$ /CTAB with Native Ferredoxin.

	$k_{\text{red.}}$ ^{a)} ($M^{-1}\cdot s^{-1}$)	k_2K_2 ^{b)} ($M^{-1}\cdot s^{-1}$)	$E^{1/2}$ (V)	k_2 (s^{-1})	K_2 (M^{-1})	acceptor
$\underline{3}$ /CTAB	3.4×10^5 ^{b)}	4.6×10^3 ^{b)}	0.04	0.82	5550	$\underline{5}$
native Fd	2.3×10^5 ^{c)}	1.6×10^3 ^{d)}	0.16	2.68	597	Co(en)_3^{3+}
		6.7×10^7 ^{e)}	ca. 0.3	ca. 10^3	6.7×10^4	cytochrome c_3

a) The reduction rates of Fe-S cluster by $\text{SO}_2^{\cdot-}$. b) Limiting second order rate constants at low reagent concentration, e.g., $k_{\text{red.}} = k_1(nK_1/M_T)^{1/2}$ and k_2K_2 , pH 8.5, 25°C, 5 mM CTAB, 100 mM Tris-Cl. c) ref. 20) d) ref. 21) e) ref. 22)

These results demonstrate that the present synthetic Fe-S cluster shows the efficient electron uptake-release activities comparable to those of native ferredoxin and, at the same time, indicate that, for the further high efficiency of the electron transfer, the topological relationships between the cluster and the electron acceptor and/or donor such as the distance and orientation are necessary to be optimized.

Experimental

General Procedure and Materials

All manipulations, except the preparations of substrate ($\underline{5}$) and N-octadecanoyl-L-cysteine($\underline{2}$), were carried out under the argon atmosphere by using a dry-box in which the concentration of oxygen was controlled to be less than 2 ppm. DMF, THF and pyridine were distilled from CaH_2 , sodium and BaO, respectively. $(n\text{-Bu}_4\text{N})_2[\text{Fe}_4\text{S}_4(\text{SBu-t})_4]$ ($\underline{1}$) was prepared according to the literature.²⁾ Other chemicals were commercially available and were not further purified.

Apparatus and Physical Measurements

$^1\text{H-NMR}$ spectra were recorded on a JEOL FX-90Q spectrometer. The chemical shifts were given in δ values from TMS or TSP. IR spectra were obtained using a Hitachi Model 215 spectrophotometer. Electronic absorption spectra were measured with a Union Giken high sensitivity spectrophotometer SM401 thermostated at $25.0 \pm 0.1^\circ\text{C}$ by attaching to a circulation system, Neslab Instruments Inc. RTE-9. Fluorescence intensities were monitored by a Shimadzu RF-503A also thermostated. Cyclic voltammetry measurements were performed with a Bioanalytical Systems Inc. CV-1B using a Hg electrode in aqueous micellar solution and a Pt electrode in DMF solution containing 0.1M of KCl and 0.1M of $n\text{-Bu}_4\text{NBr}$ as supporting electrolytes, respectively and a KCl-saturated Ag/AgCl electrode was used as a reference. Specific rotatory power was measured with a Yanako Automatic Polarimeter OR-50. Mass spectra were obtained with a JEOL JMS-DX300 mass spectrometer. Elemental analysis of metal was carried out using an atomic absorption spectrophotometer Nippon Jarrell Ash AA-8500.

N-Octadecanoyl-L-cysteine (2)

The compound (2) was prepared according to the method similar to the previous report.²³⁾ Mass spectrum; m/e , M^+ =387. Specific rotatory power; $[\alpha]_{589}^{30} = +16.0^\circ$ (benzene).

 $(n\text{-Bu}_4\text{N})_2[\text{Fe}_4\text{S}_4((\text{L})\text{-SCH}_2\text{CH}(\text{CO}_2\text{Na})\text{NHCOC}_{17}\text{H}_{35}\text{-}n)_4]$ (3)

This Fe-S cluster was prepared by a ligand exchange reaction.¹¹⁾ The sodium salt (2(a)) of 2 was prepared by treating a solution of 20 mg (5.2×10^{-5} mol) of 2 in 5 mL of ethanol with a stoichiometric amount of 0.01 N aqueous NaOH (5.2 mL). After the solvent was removed in vacuo, 12 mg (1.0×10^{-5} mol) of 1 dissolved in the 5 mL of DMF was added to the residual white crop. The mixture was stirred for 2h at 50°C, then the solvent was removed in vacuo at room temperature. The yellow-black residue obtained was dissolved in 2 mL of THF. To the mixture was added 5 mL of n-hexane, and the solution was stored at -20°C overnight. The precipitates formed were collected by filtration, washed with cold THF-hexane (20/80 (v/v)) (-20°C, 2×0.5 mL) and dried in vacuo to yield 16 mg (63 %) of 3 which was found to be a tetrahydrate by elemental analyses. $^1\text{H-NMR}$ (TSP-DMSO- d_6); δ 13.2-14.7 (m, 8H, SCH₂), 7.3 (d, 4H, NH), 5.0 (m, 4H, CH for ligand), 3.3 (m, 16H, α -CH₂ for n-Bu₄N), 2.2 (bs, 8H, COCH₂ for ligand), 0.9-1.7 (m, 132H for C₁₆H₃₃-n of ligand and 56H for β -CH₂, γ -CH₂, CH₃ for n-Bu₄N). Elemental analyses; calcd for C₁₁₆H₂₂₈N₆O₁₂S₈Na₄ Fe₄·4H₂O, C:54.77, H:9.35, N:3.30, Fe:8.78. Found, C:54.16, H:8.79, N:3.10, Fe:9.04.

 $(n\text{-Bu}_4\text{N})_2[\text{Fe}_4\text{S}_4((\text{L})\text{-SCH}_2\text{CH}(\text{CO}_2\text{Na})\text{NHAc})_4]$ (4)

This Fe-S cluster was prepared in the same method mentioned above by using L-HSCH₂CH(CO₂Na)NHAc as the ligand. To the 8.0 mg of sodium salt (2(b)) of N-acetyl-L-cysteine (4.3×10^{-5} mol) in 2 mL of DMF was added 12.0 mg of 1 (1.0×10^{-5} mol). The mixture was stirred for 2h at 50°C, then concentrated to 0.5 mL of volume in vacuo at room temperature. After the addition of 2 mL of THF, the mixture was stored at -20°C overnight. The yellow-black crystalline precipitate was collected by filtration, washed with cold THF (-20°C, 2×0.5 mL) and dried in vacuo to yield ca. 10 mg (67 %) of 4. $^1\text{H-NMR}$ (TSP-DMSO- d_6); δ 13.0-15.6 (m, 8H, SCH₂), 7.3 (d, 4H, NH), 4.9 (m, 4H, CH for ligand), 3.2 (m, 16H, α -CH₂ for n-Bu₄N), 2.0 (s, 12H, Ac), 1.6 (m, 16H, β -CH₂ for n-Bu₄N), 1.3 (m, 16H, γ -CH₂ for n-Bu₄N), 1.0 (bs, 24H, CH₃ for n-Bu₄N).

N-9-acridinyl-pivalamide (5)

To the 100 mg of 9-aminoacridine (0.52 mmol) in 5 mL of dry pyridine was added the 72 mg of trimethylacetyl chloride (0.60 mmol) slowly at room temperature. The mixture was heated to 80°C for 30 min, then the solvent was removed in vacuo at room temperature, and aqueous Na₂CO₃ was added to the residue, followed by CH₂Cl₂ extraction. The CH₂Cl₂ extract was dried over MgSO₄ and evaporated to give a crude 5. Purification by recrystallization (CHCl₃) afforded 62 mg (43 %) of the pale yellow crystallites of 5. M.P. 218-220 Mass spectrum; m/e , M^+ =278, $^1\text{H-NMR}$ (TMS-DMSO- d_6); δ 7.4-8.3 (m, 9H, ring protons and NH), 1.6 (s, 9H, CH₃). Ir (KBr); 3460, 3160, 2950, 1650, 1640, 1470 cm⁻¹.

Preparation of Aqueous Micellar Solutions

All solutions used were prepared in a carefully deoxygenated dry-box and the kinetic measurements were carried out under the argon atmosphere. To a stirred aqueous buffer solution (4 mL, 0.1 M Tris-Cl, pH 8.5) containing a cetyltrimethylammonium bromide (CTAB, 0.02 mmol), was added a 50 μL of DMF solution containing Fe-S cluster (0.04-0.24 μmol) and/or substrate (0.1-2.0 μmol) at room temperature.

The dark brown solution was filtered through the 0.45 μm membrane filter (Sartorius SM-11306) and the resulting solution was used immediately for the physical and kinetic measurement (final concentrations; CTAB 5 mM, Tris-Cl 100 mM, Fe-S cluster 0.01-0.06 mM, substrate 0.025-0.5 mM). Other aqueous micellar solutions were prepared in the similar manner.

Kinetic Measurements

In a typical experiment, the reaction was initiated by addition of 0.4 mL of the aqueous solution containing dithionite (6.0 mM) and Tris-Cl (100 mM, pH 8.5) to 2.0 mL of aqueous micellar solution containing 3 (0.036 mM), 5 (0.06 mM), CTAB (6 mM) and Tris-Cl (100 mM, pH 8.5), through the "syringe stopped flow" apparatus.²⁴⁾ The reactions were followed by monitoring the decrease of the characteristic absorption intensity at 385 nm and independently the decrease of the fluorescence at 450 nm (excit. 360 nm) observed for 5. The curve fitting analysis was performed by the standard damping Gauss-Newton method using a personal computer.

Appendix

The rate expression used in this work, eq. 1, is derived from Scheme 3 as follows.

According to the standard theory of the noncooperative multiple binding,²⁵⁾²⁶⁾ the total concentrations of the CTAB micelles (M_T), the cluster (C_T), dithionite ion (D_T) and acridine, 5, (A_T) are expressed by eq. 2, 3, 4 and 5, respectively, assuming the low concentration of $\text{SO}_2^{\cdot-}$ (D^*) species compared with others.

$$M_T = \sum_{i=0}^n \sum_{j=0}^m M(i, j) = (M + M^{2-} + M^{3-}) (1 + K_1 D_f)^n (1 + K_2 A_f)^m \quad \text{eq. 2}$$

$$C_T = M_T - \sum_{i=0}^n \sum_{j=0}^m M D_i A_j = (M^{2-} + M^{3-}) (1 + K_1 D_f)^n (1 + K_2 A_f)^m \quad \text{eq. 3}$$

$$D_T = D_f + \sum_{i=1}^n \sum_{j=0}^m i M(i, j) = D_f + n K_1 D_f (M + M^{2-} + M^{3-}) (1 + K_1 D_f)^{n-1} (1 + K_2 A_f)^m \quad \text{eq. 4}$$

$$A_T = A_f + P + \sum_{i=0}^n \sum_{j=1}^m j M(i, j) = A_f + P + m K_2 A_f (M + M^{2-} + M^{3-}) (1 + K_1 D_f)^n (1 + K_2 A_f)^{m-1} \quad \text{eq. 5}$$

$$(M(i, j) = M D_i A_j + M^{2-} D_i A_j + M^{3-} D_i A_j)$$

Here, M , D_f , A_f and P denote the micellar particle containing no cluster, free dithionite, free acridine and reduced acridine, respectively.

The total rate of the formation of M^{3-} species (X) and the initial rate of the formation of P ($A_T \gg P$) are given by eq. 6 and 7, respectively.

$$\begin{aligned} dX/dt &= k_1 \sum_{i=1}^n \sum_{j=0}^m (M^{2-} D_{i-1} A_j D^*) - k_2 \sum_{i=0}^n \sum_{j=1}^m j M^{3-} D_i A_j \\ (X &= \sum_{i=0}^n \sum_{j=0}^m (M^{3-} D_i A_j)) \end{aligned} \quad \text{eq. 6}$$

$$dP/dt = k_2 \sum_{i=0}^n \sum_{j=1}^m j M^{3-} D_i A_j \quad \text{eq. 7}$$

Since the concentration of $\text{SO}_2^{\cdot-}$ is confirmed by the ESR measurement not to largely change by addition of CTAB, the dissociation constant of dithionite in the micelles is assumed to be same with that in the bulk aqueous solution, i.e.,

$$K_d = (D_T^{\cdot})^2 / D_T^b \quad \text{eq. 8}$$

where the subscript T and superscript b denote the total concentration and the species bound on the micelles, respectively. Therefore, D_T^b and D_T^{*b} are estimated by eq. 9 which is derived from eq. 2, 4 and 8.

$$D_T^b = D_T - D_f = nK_1 D_f M_T / (1 + K_1 D_f) \text{ and } D_T^{*b} = (K_d D_T^b)^{1/2} \quad \text{eq. 9}$$

Since the probability of the formation of D^* in one micellar particle is proportional to its number of bound dithionite, the concentration of $M^{2-D_{i-1}A_j}D^*$ is given as follows.

$$M^{2-D_{i-1}A_j}D^* = (D_T^{*b}/D_T^b) iM^{2-D_{i-1}A_j} \quad \text{eq. 10}$$

Then, the eq. 6 was transformed in eq. 11 by using eq. 3 and 10.

$$dX/dt = k_1 \left(\frac{nK_1 K_d D_f}{M_T (1 + K_1 D_f)} \right)^{1/2} (C_T - X) - k_2 \frac{mK_2 A_f}{1 + K_2 A_f} X \quad \text{eq. 11}$$

Assuming the steady state condition for the highly active M^{3-} species (X), eq. 1 is obtained from eq. 7.

References and Notes

- 1) Hall, D. O., Evans, M. C. W., Nature, 1969, 223, 1342.
- 2) Averill, B. A., Herskovitz, T., Holm, R. H., Ibers, J. A., J. Am. Chem. Soc., 1973, 95, 3523.
- 3) Berg, J. M., Holm, R. H., "Iron-Sulfur Proteins", 1983, Spiro, T. G., Ed., Wiley-Interscience, N.Y., Vol. IV, Cap. 1.
- 4) a) Itoh, T., Nagano, T., Hirobe, M., Tet. Lett., 1980, 21, 1343.
b) Tanaka, K., Tanaka, M., Tanaka, T., Chem. Lett., 1981, 895.
c) Tezuka, M., Yajima, T., Tsuchiya, A., Matsumoto, Y., Uchida, Y., Hidai, M., J. Am. Chem. Soc., 1982, 104, 6834.
d) Inoue, H., Sato, M., J. Chem. Soc., Chem. Commun., 1983, 983.
e) Ueyama, N., Sugawara, T., Kajiwara, A., Nakamura, A., J. Chem. Soc., Chem. Commun., 1986, 434.
- 5) Tsai, H., Sweeney, M. V., Coyle, C. L., Inorg. Chem., 1985, 24, 2796.
- 6) Only one example of the application of the synthetic cluster to electron transfer catalyst in the aqueous solution has been reported by using dithionite as the electron donor and native hydrogenase as the final electron acceptor. The detailed mechanism, however, was not known. see Adams, M. W. W., Reeves, S. G., Hall, D. O., Christou, G., Ridge, B., Rydon, H. N., Biochem. Biophys. Res. Commun., 1977, 79, 1184.
- 7) a) Bruice, T. C., Maskiewicz, R., Job, R. C., Proc. Nat. Acad. Sci. USA, 1975, 72, 231.
b) Job, R. C., Bruice, T. C., Proc. Nat. Acad. Sci. USA, 1975, 72, 2478.
- 8) a) Maskiewicz, R., Bruice, T. C., Bartsch, R. G., Biochem. Biophys. Res. Commun., 1975, 65, 407.
b) Lode, E. T., Murray, C. L., Rabinowitz, J. C., J. Biol. Chem., 1976, 251, 1675.
c) Maskiewicz, R., Bruice, T. C., Proc. Nat. Acad. Sci. USA, 1977, 74, 5231.
- 9) Tabushi, I., Kuroda, Y., Sasaki, Y., Tet. Lett., 1986, 27, 1187.
- 10) Tabushi, I., Kuroda, Y., Sasaki, Y., J. Chem. Soc., Chem. Commun., 1987, 1622.

- 11) Bobrik, M. A., Que, Jr., L., Holm, R. H., J. Am. Chem. Soc., 1974, 96, 285.
- 12) Hill, C. L., Renaud, J., Holm, R. H., Mortenson, L. E., J. Am. Chem. Soc., 1977, 99, 2549.
- 13) Stephens, P. J., Thomson, A. J., Dunn, J. B. R., Keiderling, T. A., Rawlings, J., Rao, K. K., Hall, D. O., Biochemistry, 1978, 17, 4770.
- 14) Tanaka, K., Moriya, M., Tanaka, T., Inorg. Chem., 1986, 25, 835.
- 15) DePamphilis, B. V., Averill, B. A., Herskovitz, T., Que, Jr., L., Holm, R. H., J. Am. Chem. Soc., 1974, 96, 4159.
- 16) Tabushi, I., Kuroda, Y., Sasaki, Y., Tet. Lett., 1987, 28, 4069.
- 17) Since the original reported value of k was $2200 \pm 300 \text{ M}^{-1/2} \cdot \text{s}^{-1}$ which contained micellar concentration term as the form $k_1/\sqrt{M_T}$ (see Appendix), the value shown in this paper was corrected by multiplying $\sqrt{M_T}$ to afford the true $k_1 (\text{s}^{-1})$.
- 18) The initial value of D_f and A_f are calculated from following equations (see ref. 25 and Appendix),
- $$D_f = ((K_1 D_T - nK_1 M_T - 1) + ((K_1 D_T - nK_1 M_T - 1)^2 + 4K_1 D_T)^{1/2}) / 2K_1$$
- $$A_f = ((K_2 A_T - mK_2 M_T - 1) + ((K_2 A_T - mK_2 M_T - 1)^2 + 4K_2 A_T)^{1/2}) / 2K_2$$
- where D_T and A_T are initial (total) concentrations of dithionite and A (substrate, 5), respectively.
- 19) The concentration of CTAB micelles was calculated by assuming the aggregation number and CMC to be 61 and 0.9 mM, respectively, see Fendler, J. H., Fendler, E. J., "Catalysis in Micellar and Macromolecular Systems", 1975, Academic Press, New York.
- 20) Lambeth, O. D., Palmer, G., J. Biol. Chem., 1973, 248, 6095.
- 21) Armstrong, F. A., Sykes, A. G., J. Am. Chem. Soc., 1978, 100, 7710.
- 22) Capeiller-Blandin, C., Guerlesquin, F., Bruschi, M., Biochim. Biophys. Acta., 1986, 848, 279.
- 23) Heitmann, P., Eur. J. Biochem., 1968, 3, 346.
- 24) Tabushi, I., Nishiya, T., Yagi, T., Inokuchi, H., J. Am. Chem. Soc., 1981, 103, 6963.
- 25) Tanford, C., "Physical Chemistry of Macromolecules", 1961, John Wiley & Sons, N. Y., Cap. 8.
- 26) The theory gives following two general relationships for X and Y (see ref. 25)
- $$\sum_{i=0}^n XY_i = X(1+KY_f)^n \quad \text{and} \quad \sum_{i=0}^n iXY_i = nKXY_f(1+KY_f)^{n-1}$$